SCIENTIFIC REPORTS

OPEN

SUBJECT AREAS:

ATOMIC AND MOLECULAR INTERACTIONS WITH PHOTONS

QUANTUM OPTICS

SLOW LIGHT

Received
4 June 2013

Accepted
19 December 2013

Published
3 February 2014

Correspondence and requests for materials should be addressed to M.A. (artoni@lens.unifi.it)

Manipulating Frequency-Bin Entangled States in Cold Atoms

A. Zavatta[1,2], M. Artoni[1,2,3], D. Viscor[4] & G. La Rocca[5]

[1]Istituto Nazionale di Ottica (INO-CNR), Firenze, Italy, [2]European Laboratory for Nonlinear Spectroscopy, Firenze, Italy, [3]Department of Engineering and Information Technology, Brescia University, Brescia, Italy, [4]Departament de Física, Universitat Autònoma de Barcelona, E-08193 Bellaterra, Spain, [5]Scuola Normale Superiore and CNISM, Pisa, Italy.

Optical manipulation of entanglement harnessing the frequency degree of freedom is important for encoding of quantum information. We here devise a phase-resonant excitation mechanism of an atomic interface where full control of a narrowband single-photon two-mode frequency entangled state can be efficiently achieved. We illustrate the working physical mechanism for an interface made of cold ^{87}Rb atoms where entanglement is well preserved from degradation over a typical 100 μm length scale of the interface and with fractional delays of the order of unity. The scheme provides a basis for efficient multi-frequency and multi-photon entanglement, which is not easily accessible to polarization and spatial encoding.

The advent of optical quantum information processing has placed stringent requirements on the ability to handle nonclassical states such as single-photon and entangled states. At variance with weak coherent light beams, which can also be used as pseudo–photon sources, single-photon Fock states either on demand or heralded guarantee conditional security, *e.g.*, in quantum cryptography[1] and are crucial in optical information processing[2–5]. Single-photon entangled states, in particular, can be generated and employed, *e.g.*, for teleportation[6] and linear optics quantum computation[7]. This is a basic form of entanglement and it is in principle isomorphic to any other kind of two-photon entanglement[8,9].

Single-photon *spatial* entanglement, *e.g.*, is attained by splitting a single-photon Fock state on a 50/50 beam splitter. Because the photon itself cannot be split, quantum mechanics prescribes that the photon must take both paths at once, thereby entangling the two spatial modes at the outputs of the beam-splitter. Such a single-photon entangled state realizes an optical qubit, where information can be encoded. Single-photon *frequency* entanglement can also be exploited to realize frequency qubit encoding[10], which uses discrete orthogonal modes in the frequency domain rather than spatial modes. This kind of encoding appears more suitable to multi-mode entanglement[11,12] and quantum information can benefit from multi-frequency encoding in much the same way as classical communication has from the introduction of frequency multiplexing.

We here show that single-photon frequency entanglement can be efficiently controlled trough an interface made of an optically dense sample of cold atoms. This would be crucial toward the realization of quantum memories that work with single-photon multimode entangled states[2]; in the following we specifically illustrate the case of a single-photon *two-mode* frequency entangled state of the form,

$$|\Phi_e\rangle = \frac{1}{\sqrt{2}}\left(|0_m,1_p\rangle + e^{i\phi_\eta}|1_m,0_p\rangle\right). \quad (1)$$

The photon excitation is simultaneously shared by *two* atomic transitions of frequency ω_p and ω_m (See Fig. 1), with $|0_m, 1_p\rangle$ and $|1_m, 0_p\rangle$ being the states with the photon created in one or the other frequency mode, whose phase relation should remain fixed to preserve entanglement through the interface. The state $|\Phi_e\rangle$, an archetype of frequency entanglement, can be conditionally generated by standard techniques using parametric downconversion where a crystal with $\chi^{(2)}$ nonlinearity is pumped at two different frequencies[13]. A signal and idler photon pair is generated in two different spatial directions and detection of one idler photon heralds the presence of a photon along the signal path. Indistinguishability between which pump has generated the photon pair leads to the superposition state (1), with the two possible alternatives of a single-photon with frequency ω_m and ω_p and with a relative phase ϕ_η set by the generation scheme. It is worth noting that standard optical manipulations can be used to convert $|\Phi_e\rangle$ into a familiar single-photon spatialmode entangled state, namely through a unitary operation which redefines the state into a truly nonlocal entanglement[14].

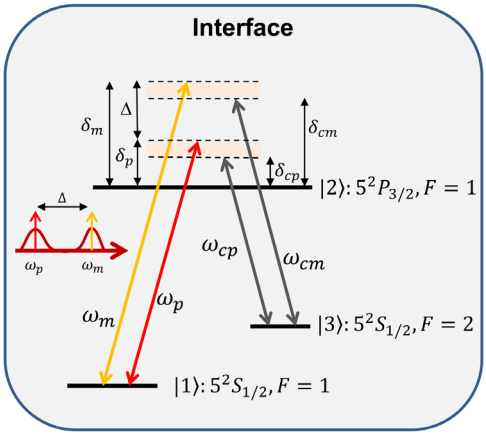

Figure 1 | Atomic interface for a single-photon frequency-bin entangled state. A sample of cold atoms loaded into a magneto-optical trap (MOT) and initially pumped to state $|1\rangle$ is used as interface. Two continuous strong coupling beams ω_{cm} and ω_{cp}, with the same polarization and Rabi frequency Ω_c but different detunings from the excited state $|2\rangle$, control the coupling of the frequency entangled state (1) to the interface. The relevant wavepacket of length $\mathcal{L}$ and bandwidth such that $c/\mathcal{L} \lesssim \gamma_2 \ll \Delta$ is double Λ-resonant with the coupling beams ($\omega_m - \omega_{cm} = \omega_p - \omega_{cp}$) through a nearly-resonant ($\delta_p \lesssim \gamma_2$) and a far off-resonant ($\delta_m \gg \delta_p$) (Raman) transition between the two hyperfine electronic ground states $|1\rangle$ and $|3\rangle$. Under such conditions non-resonantly excited coherences[30] can be neglected and control of the entangled state is described by the closed set of coupled equations (2–3). The energy level scheme corresponds to the D_2 line in ^{87}Rb ($5^2S_{1/2} \rightarrow 5^2P_{3/2}$) with a transition wavelength $\lambda_{21} = 780.24$ nm. Hyperfine ground state dephasing and excited state relaxation rate are $\gamma_3 = 2\pi \times 1$ kHz and $\gamma_2 = 2\pi \times 6$ MHz.

Routing the entangled state (1) requires a very good degree of control over the photon propagation and most importantly over the photon's quantum state. Routing has to preserve entanglement, in fact, and should perform sufficiently large and flexible delays to be useful in all-optical processing. We show that this can be achieved through a phase-resonant excitation mechanism of an atomic interface where the two constraints above can be satisfied. The mechanism mainly relies, in contrast to previous studies[15], on dark-state matching effects which make our single-photon two-mode frequency entangled state particularly easy to control.

The underpinning features of the interface can be understood by considering an ultracold sample of N atoms placed at random positions in a volume V in the three-level double-Λ interaction scheme[16] described in Fig. 1. The interface coupling dynamics is studied by considering for each of the two frequency-bins a *weak* quasi-monochromatic field with mean frequency ω_m and ω_p and corresponding wave-number k_m and k_p. In the plane-wave representation the *field* amplitude operator $\hat{E}_m^+(z,t)$ comprises a finite number of modes each described by Heisenberg photon annihilation operators[17]. In such a narrow-band approximation and to the lowest order in the (weak) field this is found to obey the equation of motion,

$$\left(\frac{1}{c}\frac{\partial}{\partial t} + \frac{\partial}{\partial z}\right)\hat{E}_m^+(z,t) \simeq -i\frac{A_o\omega_{21}}{\tilde{\delta}_m}\hat{E}_m^+(z,t) + \frac{A_1\omega_{21}}{\tilde{\delta}_m}\frac{\hbar\Omega_{cm}}{2}\hat{\pi}_S(z,t)e^{i(\kappa_{cm}z-\omega_{cm}t)}, \quad (2)$$

where $\tilde{\delta}_m = \delta_m + i\gamma_2 = \omega_m - \omega_{21} + i\gamma_2$ is the complex detuning expressed in terms of the excited state decay rate (γ_2) while $A_o = (N/V)\times(\hat{\epsilon}\cdot\boldsymbol{d}_{12})^2/2\epsilon_o\hbar_C = A_1\times(\hat{\epsilon}\cdot\boldsymbol{d}_{12})$, with $\boldsymbol{d}_{12}$ the electric-dipole matrix element between the states $|1\rangle$ and $|2\rangle$. A similar result obtains for the other mode operator $\hat{E}_p^+(z,t)$. The two fields are taken here with the same polarization ($\hat{\epsilon}$). The operator $\hat{\pi}(z,t)$ on the right hand side of (2) describes a collective atomic excitation and can likewise be expressed in terms of a quasi-monochromatic plane-wave expansions of *atomic* Heisenberg operators. The relevant evolution equation is,

$$i\hbar\frac{\partial}{\partial t}\hat{\pi}(z,t) \simeq \left\{\left(\frac{\hbar\tilde{\omega}_{31}}{2} + \frac{\hbar|\Omega_{cm}|^2}{4\tilde{\delta}_m}\right)\hat{\pi}(z,t) - i\frac{\Omega_{cm}^*(\hat{\epsilon}\cdot\boldsymbol{d}_{12})}{2\tilde{\delta}_m}\hat{E}_m^+(z,t)e^{-i(\kappa_{cm}z-\omega_{cm}t)}\right\} + \{m\leftrightarrow p\}, \quad (3)$$

where $\tilde{\delta}_p = \delta_p + i\gamma_2 = \omega_p - \omega_{21} + i\gamma_2$ and $\tilde{\omega}_{31} = \omega_{31} - i\gamma_3$ is expressed in terms of the two hyperfine ground levels dephasing (γ_3). The last term within brackets is obtained from the previous one with the interchange $m \leftrightarrow p$. Upon Fourier transforming (2–3) in time one is left with a set of coupled eq.s describing the spatial evolution of the two modes amplitude operators $\hat{E}_m^+(z,\omega)$ and $\hat{E}_p^+(z,\omega)$ inside the interface. In particular, these eq.s contain on the right hand side of $\partial\hat{E}_m^+(z,\omega)/\partial z$ and $\partial\hat{E}_p^+(z,\omega)/\partial z$ both *self-coupling* and *cross-coupling* terms. The former basically represent the propagation of each field mode in the presence of the corresponding coupling beam, as for a typical Λ-configuration supporting electromagnetically induced transparency[18]. The latter terms originate instead from the interaction between the far-detuned and the nearly resonant field mode (Cf. Fig. 1). Solutions of these coupled eq.s yield $\hat{E}_m^+(z,\omega)$ and $\hat{E}_p^+(z,\omega)$; upon converting back to the time-domain the resulting amplitude operators $\hat{E}_m^+(z,t)$ and $\hat{E}_p^+(z,t)$ can be rewritten in terms of the corresponding free-space operators $\hat{E}_m'^+(z,t)$ and $\hat{E}_p'^+(z,t)$ as,

$$\begin{pmatrix}\hat{E}_m^+(z,t)\\ \hat{E}_p^+(z,t)\end{pmatrix} = \begin{pmatrix}\mathcal{E}_{mm}\left(\tilde{\delta}_m,z\right) & e^{i\Delta\phi_c}e^{i\frac{\Delta}{c}(z-ct)}\mathcal{E}_{mp}\left(\tilde{\delta}_p,z\right)\\ e^{-i\Delta\phi_c}e^{-i\frac{\Delta}{c}(z-ct)}\mathcal{E}_{pm}\left(\tilde{\delta}_m,z\right) & \mathcal{E}_{pp}\left(\tilde{\delta}_p,z\right)\end{pmatrix}\begin{pmatrix}\hat{E}_m'^+(z,t)\\ \hat{E}_p'^+(z,t)\end{pmatrix}. \quad (4)$$

Similar operators transformation (4) have been used in investigations of quantum optical properties of parametric processes in atomic media such as amplification enhancement[19], mirrorless oscillations[20], quantum noise and correlations in wave mixing[21], efficient single-photon frequency switching and entangled state generation[15], just to mention a few.

Here we use instead (4) to discuss a phase-resonant mechanism to control and especially to preserve the frequency-bin entangled state (1) through the interface of Fig. 1. It should be noted that in general the propagation of one field excitation that is shared between two atomic frequency transitions naturally tends to contaminate the quality of the entanglement. Two frequency modes sufficiently separated from one another may exhibit in fact appreciably different dispersion and absorption. In addition, the two coupling beams, each separately coupled to the two frequency components of the single-photon, naturally triggers a mode mixing which further spoils entanglement.

Results

The four complex amplitudes $\mathcal{E}$'s in (4) determine the evolution of the photon's electric field through the interface. The evolution depends, in particular, on the lasers initial relative phase $\Delta\phi_c$ as expected for a closed-loop excitation structure where the two modes interact through a common spin-coherence. Each amplitude's expression is rather involved, yet for nearly resonant Raman transitions ($\delta_p \simeq \delta_{cp}$ and $\delta_m \simeq \delta_{cm}$) and in the limit of Raman detunings for which $\Delta \gg \{\delta_p, \gamma_2\}$, the overall space-dependence of $\mathcal{E}_{mp}$ can be rewritten ($\delta_{cp} = 0$, $\delta_{cm} = \Delta$) as a superposition of two waves,

$$\mathcal{E}_{mp} \simeq \frac{1}{2}\left\{e^{i(n_- - 1)\frac{\omega_p z}{c}} - e^{i(n_+ - 1)\frac{\omega_p z}{c}}\right\} \quad (5)$$

and similarly for

$$\mathcal{E}_{pp} \simeq \frac{1}{2}\left\{e^{i(n_- -1)\frac{\omega_p z}{c}} + e^{i(n_+ -1)\frac{\omega_p z}{c}}\right\} \tag{6}$$

where the detuning and space dependences have been conveniently omitted on purpuse. We denote by

$$n_- \simeq 1 - \frac{A_o c}{2}\frac{\delta_p + i\gamma_3}{\tilde{\delta}_p(\delta_p + i\gamma_3) - (\Omega_c/2)^2} \tag{7}$$

and

$$n_+ \simeq 1 - \frac{2A_o c}{\tilde{\delta}_p + \Delta} \tag{8}$$

the complex refractive index exhibited by the atomic interface respectively on the nearly-resonant transition and on the far-detuned Raman transition (See Fig. 1). The remaining matrix terms $\mathcal{E}_{pm}$ and $\mathcal{E}_{mm}$ in (4) can be shown to obtain respectively from $\mathcal{E}_{mp}$ and $\mathcal{E}_{pp}$ upon a suitable replacing of $\omega_p \to \omega_m$ and $\tilde{\delta}_p \to \tilde{\delta}_m - \Delta$.

The evolution of the frequency-bin entanglement, on the other hand, is studied by seeking the conditions under which the initial state (1) maintains the form,

$$|\Phi_e\rangle \to a_p(z,t)|0_m, 1_p\rangle + a_m(z,t)|1_m, 0_p\rangle, \tag{9}$$

with the entanglement clearly being preserved when the two amplitudes in (9) remain equal to those in (1). The evolution hinges on the space-time dependence of the complex amplitudes $a_p(z, t)$ and $a_m(z, t)$ and this is what we now compute. The square magnitude $|a_p(z, t)|^2$ represents the normal-ordered averaged Poynting vector $S_p(z, t) = \langle\Phi_e| : S_p(z, t) : |\Phi_e\rangle$ in the mode p across the interface, scaled to the single-photon incident pulse peak power density S_o. Similarly for $|a_m(z, t)|^2$. The field correlators required to obtain $S_m(z, t)$ and $S_p(z, t)$[22] are computed using the fact that at some given reference time (t) across an interface the expectation values are independent of the representation. For a single-photon wavepacket of length $\mathcal{L}$ and with a Gaussian frequency distribution $\xi_{m,p}(\omega) = \left(\mathcal{L}^2/2\pi c^2\right)^{1/4} e^{-\mathcal{L}^2(\omega-\omega_{m,p})/4c^2}$ one obtains after some lengthily algebra,

$$S_{\substack{m\\p}}(z,t) \simeq \frac{S_o}{2}\left|\mathcal{E}_c^-(z,t) \mp i\mathcal{E}_s^+(z,t)e^{i\delta(z)\pm 2i\zeta}\right|^2. \tag{10}$$

where the upper and lower signs denote specifically $S_o \times |a_m(z, t)|^2$ and $S_o \times |a_p(z, t)|^2$. Evolution of the entanglement hinges on the *interference* of the two envelopes,

$$\mathcal{E}_c^-(z,t) = \cos\Phi \times e^{-\kappa - \omega_p z/c} e^{-\left(z - v_g^- t\right)^2/\left(\mathcal{L}v_g^-/c\right)^2} \tag{11}$$

and

$$\mathcal{E}_s^+(z,t) = \sin\Phi \times e^{-\kappa + \omega_p z/c} e^{-\left(z - v_g^+ t\right)^2/\left(\mathcal{L}v_g^+/c\right)^2}. \tag{12}$$

These are modulated Gaussians propagating at different group velocities $v_g^{\pm}$, damping over different length scales and subject, in addition, to an important (out-of-phase) modulation with a phase $\Phi \simeq \left(\Delta\phi_c - \phi_\eta\right)/2$.

Interference can easily be controlled *both* through this external phase and through the internal optical response of the atoms, respectively, through the couplings relative phase ($\Delta\phi_c$) and through the real ($\eta_\pm$) and imaginary ($\kappa_\pm$) parts of $n_\pm$ in (7–8). The medium response controls, in particular, the phase $\delta(z) \simeq \left(\eta_+ - \eta_-\right)\omega_p z/c$ of the interference term in (10), responsible for photon swapping between the two modes.

We first illustrate a situation, a main point in our proposal, where the interface can be tuned to avoid degradation of the state (1). The frequency-bin entangled state (1) remains largely unspoiled, in fact, for a vanishing (pulse) detuning δ_p and for coupling beams relative phases such that $\Delta\phi_c - \phi_\eta = 2n \times \pi$, as shown in Fig.s 2a. This corresponds to a phase Φ for which $\mathcal{E}_s^+(z,t) \to 0$ in (10). Physically, this arises from the matching of dark states, and can be understood supposing that each component of the entangled state creates its own dark state through the corresponding coupling beam. When the two dark states exactly match to one another the atoms will loosely couple to the two field modes leading to a regime of reduced absorption and slow-light propagation (Fig. 2a). For coupling beams of the same intensities this occurs[23] for a photon Rabi frequencies such that $\Omega_p = \Omega_m$ and under the (four-photon) resonance condition $\omega_m - \omega_{cm} = \omega_p - \omega_{cp}$, both clearly met here. Within such a regime the entangled wavepacket can be delayed up to nearly 5 times the temporal width (τ) with negligible losses over a 500 μm long interface. This amounts to fractional delays - the ratio between the absolute delay $\sim L/v_g^-$ and the pulse width τ - of the order of 5 occurring with very modest absorption and pulse deformation. Dark-state matching (Fig. 2a) sets an upper bound on the actual capability to perform reversible mapping[24] of the entangled state (1). Conversely, when $\Delta\phi_c - \phi_\eta = (2n + 1) \times \pi$ the other amplitude $\mathcal{E}_c^+(z,t) \to 0$ in (9), atoms will now couple to the photon field making both modes to quickly dissipate through the sample (Fig. 2b).

We also include in the discussion a somewhat opposite situation in which the entanglement is largely spoiled. That occurs for coupling phases $\Delta\phi_c$ such that $\Delta\phi_c - \phi_\eta = (2n + 1) \times (\pi/2)$ and $\delta_p = 0$, as shown in Fig.s 2(c, d). The resulting space–time evolution of the

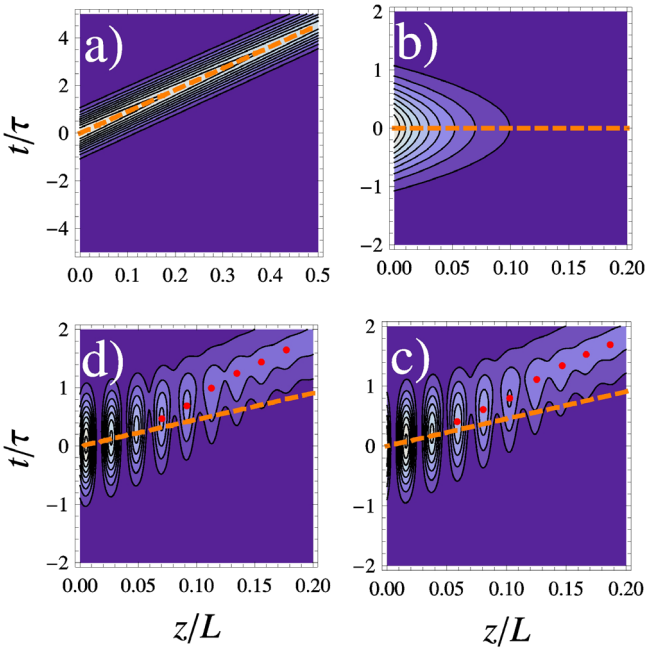

Figure 2 | Entanglement evolution. Power density distribution from (10) yielding the evolution of the single-photon frequency-bin entangled state (1) through a ^{87}Rb MOT trap of length $L = 1000$ μm and density $N/V = 5 \times 10^{13}$ cm^{-3} (See interface Fig. 1). The single-photon wavepacket has a $\tau = 5.2$ μsec long Gaussian envelope with a detuning $\delta_p = 0$ and a mode separation $\Delta = 20 \times \gamma_2$ while the Rabi frequency of the coupling beams is $\Omega_c = 2 \times \gamma_2$. Clockwise from ($a$) → ($d$) the relative phase $\Delta\phi_c - \phi_\eta$ takes respectively the values $\{0, \pi, \pi/2, \pi/2\}$. Slow evolution takes place with little absorption preserving the state (a), with quite strong damping (b) or through damped coherent spatial oscillations between mode p (c) and mode m (d). The wavepacket evolution occurs with an overall velocity (*orange dashed*) $v_g^- \simeq 21$ m/sec (a), $v_g^+ \simeq 3.3 \times 10^3$ m/sec (b) and $v \simeq 42$ m/sec (c, d). Color dots in (c,d) depict the wavepacket drift due to absorption. Note the different length scales in Fig. 2a and Fig. 2(c, d).

entangled state (9) exhibits spatial oscillations between its two frequency components with a significant damping over much shorter lengths, as we may see by comparing Fig. 2a and Fig.s 2(c, d). Such a characteristic coherent photon swapping between the two-frequency bins arises from maximum interference of the two envelopes $\mathcal{E}_c^-(z,t)$ and $\mathcal{E}_s^+(z,t)$ in (10). In spite of the different spreading of these two envelopes, the entangled state wavepacket evolves at a velocity that locks at $\upsilon \simeq 2 \times v_g^-$, as it may be directly inferred from the composition of the slow (v_g^-) and fast (v_g^+) velocities components in (10). Actual departures of the photon wavepacket overall evolution from υ are due to increasing values of the absorption with distance. Notice that *only* few times can entanglement be recovered over a typical 100 μm length scale. As inferred from (7–8) and (10), this occurs almost periodically at specific points spaced by $L_{osc} \simeq 2\pi c/\omega_p(\eta_+ - \eta_-)$. By varying L_{osc}, modifying for instance the atomic response through the pulse detuning δ_p (see eq.s 7–8), one may in principle adjust the position where entanglement is retained[15], though this is clearly not practical. For the realistic interface parameters of Fig. 2, a sizable level of decoherence due to losses seems to further prevent such a depth-dependent entanglement from maintaining the original state (1).

The three different damping situations are detailed in Fig. 3, where we plot the spatial damping of the *maximum* degree of entanglement. Notice that preserving the entanglement is rather sensitive to the pulse detuning δ_p from resonance (*dashed*).

Discussion

The present phase-resonant atomic interface mechanism requires narrowband single-photon states. Spontaneous parametric down-conversion may be a suitable candidate for the generation of the state $|\Phi_e\rangle$ in (1). Alternatively, two concomitant spontaneous Raman scattering processes may be used, namely by pumping the atomic ensemble with two pump beams of different frequencies and a fixed phase relation between them. Raman scattering is responsible for the emission of idler (*Stokes*) and signal (*anti-Stokes*) twin photons with positive and negative frequency shifts, relative to the two pumps. In the presence of *only* one pump, the observation of a photon in the idler mode would herald the emission of a signal photon with a well defined frequency, determined by the pump frequency as

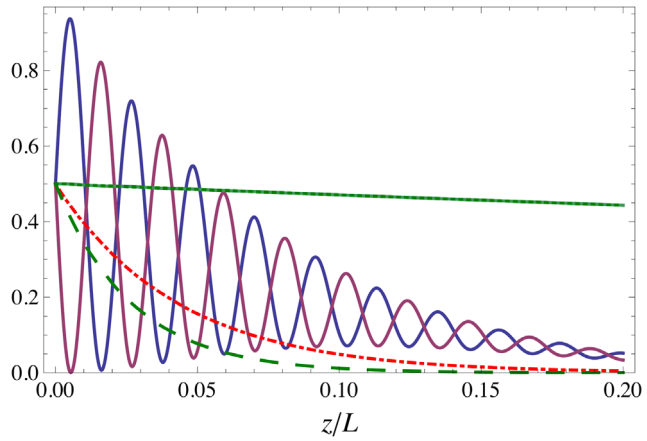

Figure 3 | Maximum entanglement distribution. Frequency-bin entangled state peak power density spatial distribution in units of S_o for the evolution profiles of Fig. 2. Each curve is plotted at a specific time t_{max} obtained from the ratio of the position z and each of the evolution overall velocities shown Fig. 2 (*orange dashed*). Green curves describe the weak damping case of Fig. 2a respectively for $\delta_p = 0$ (*solid*) and $\delta_p = 0.1 \times \gamma_2$ (*dashed*). Red curve (*dot – dashed*) describes the strong damping case of Fig. 2b, while blue and purple curves correspond to the two frequency-mode swapping intensity distribution of Fig. 2(c, d).

demonstrated in[25]. In our case, however, in which *both* pumps are present, the above emission process will occur through either pump with low but nearly equal probabilities, hence the observation of an *idler* photon heralds the emission of a *signal* single-photon. The probability of both processes occurring simultaneously is negligible for sufficiently weak coupling beams. However, the detection of the single idler photon does not reveal, even in principle, which pump has triggered the emission of the photon in the signal channel. Such an indistinguishability clearly results in the generation of the superposition state (1). The phase ϕ_η of state (1) is determined by the relative phase between the two coupling beams and can be easily adjusted to have the desired value. Such an initial phase can also be fully characterized with homodyne tomography (See *e.g.*[13,26]), prior propagation through the interface.

The main advantages of the analytical approach adopted in solving the coupled evolution eq.s (2–3) are the physical insight into the nature of a new control mechanism for a frequency-qubit and the ease in computing all different aspects of its evolution (see e.g. Fig.s 2a–2d). Following eq. (10), in fact, control of the frequency-bin entangled state hinges on the *interference* of the two modulated Gaussians envelopes $\mathcal{E}_s^+(z,t)$ and $\mathcal{E}_c^-(z,t)$ and is attained by manipulating both the internal optical response of the atoms and the (external) coupling relative phase $\Delta\phi_c$. Loss of entanglement due to absorption, dispersion and mixing intrinsic to the resonant excitation of the interface's double-lambda configuration of Fig. 1 is all embedded in the joint space-time evolution of $\mathcal{E}_s^+(z,t)$ and $\mathcal{E}_c^-(z,t)$.

Notice that the evolution of the frequency-bin entangled state is in general determined not only by the magnitude of the complex amplitudes $a_p(z,t)$ and $a_m(z,t)$ but also by their relative phase. Only in the relevant situation of Fig. 2a, can such a relative phase be shown to remain essentially constant during propagation, at variance with the situation of Fig. 2(c, d) where the two mode components accumulate steep variations of the relative phase during propagation. This further complicates the possibility of achieving depth-dependent entanglement of two Fock-states[15].

Although the present analysis has been carried out for the *single-photon* entangled state (1) control interface, the transformation (4) may also be directly used to study the case of a *two-photon* entangled state - with results that can be derived in a similar way - or to study extensions to control *multi-photons* entanglement. Extensions to control of a *multi-frequency* entangled state may also be conceived. In this case the frequency domain can be divided into several frequency bins, corresponding to different atomic transitions, where quantum information can be encoded. The interface mechanism would become an efficient control tool for multi-frequency entanglement in quantum memories based on atomic ensembles. To this extent, it should be noted that reversible mapping of multi frequency-entanglement[24] would require coherence times which are largely independent of the number of (frequency) modes. This is at variance *e.g.* with recent schemes for time-bin multimode entanglement[26,27] that are bound to work with a restricted number of time-bins. It is finally worth to emphasize that our scheme is rather general, in terms of the underlying working mechanism, though the above analysis specifically relates to a cold atoms interface[30]. It may well be adapted to other interfaces including atomic ensembles in solids such as *e.g.* crystals doped with rare-earth-metal ions[28] or with N-V color centers[29], both having a potential for developing quantum information architectures based on solid devices. Dark-state matching, in particular, is expected to remain robust providing a mean to compensate for differential dispersion and absorption also in these crystals.

1. Scarani, V. *et al.* The security of practical quantum key distribution. *Rev. Mod. Phys.* **81**, 1301–1350 (2009).
2. Simon, C. *et al.* Quantum memories. *Eur. Phys. J. D* **58**, 1–22 (2010).

3. Gouët, J.-L. L. & Moiseev, S. Quantum memory. *J. Phys. B: At. Mol. Opt. Phys.* **45**, 120201 (2012).
4. Duan, L.-M., Lukin, M. D., Cirac, J. I. & Zoller, P. Long-distance quantum communication with atomic ensembles and linear optics. *Nature* **414**, 413–418 (2001).
5. Kimble, H. J. The quantum internet. *Nature* **453**, 1023–1030 (2008).
6. Pegg, D. T., Phillips, L. S. & Barnett, S. M. Optical State Truncation by Projection Synthesis. *Phys. Rev. Lett.* **81**, 1604–1606 (1998).
7. Kok, P. *et al*. Linear optical quantum computing with photonic qubits. *Rev. Mod. Phys.* **79**, 135–174 (2007).
8. Tan, S. M., Walls, D. F. & Collett, M. J. Nonlocality of a single photon. *Phys. Rev. Lett.* **66**, 252–255 (1991).
9. Heaney, L. & Vedral, V. Natural mode entanglement as a resource for quantum communication. *Phy. Rev. Lett.* **103**, 200502– (2009).
10. Ramelow, S., Ratschbacher, L., Fedrizzi, A., Langford, N. K. & Zeilinger, A. Discrete tunable color entanglement. *Phys. Rev. Lett.* **103**, 253601 (2009).
11. Pinel, O. *et al*. Generation and characterization of multimode quantum frequency combs. *Phys. Rev. Lett.* **108**, 083601 (2012).
12. Menicucci, N. C. *et al*. Universal quantum computation with continuous-variable cluster states. *Phys. Rev. Lett.* **97**, 110501 (2006).
13. Polycarpou, C., Cassemiro, K. N., Venturi, G., Zavatta, A. & Bellini, M. Adaptive detection of arbitrarily shaped ultrashort quantum light states. *Phys. Rev. Lett.* **109**, 053602 (2012).
14. van Enk, S. J. Single-particle entanglement. *Phys. Rev. A* **72**, 064306 (2005).
15. Payne, M. G. & Deng, L. Quantum entanglement of fock states with perfectly efficient ultra-slow single-probe photon four-wave mixing. *Phys. Rev. Lett.* **91**, 123602 (2003).
16. Raczyński, A. & Zaremba, J. Controlled light storage in a double lambda system. *Opt. Commun.* **209**, 149–154 (2002).
17. Loudon, R. *The quantum theory of light* (Clarendon Press, Oxford, 2000).
18. Fleischhauer, M., Imamoglu, A. & Marangos, J. P. Electromagnetically induced transparency: Optics in coherent media. *Rev. Mod. Phys.* **77**, 633–673 (2005).
19. Lukin, M. D., Hemmer, P. R., Löffler, M. & Scully, M. O. Resonant enhancement of parametric processes via radiative interference and induced coherence. *Phys. Rev. Lett.* **81**, 2675–2678 (1998).
20. Fleischhauer, M., Lukin, M. D., Matsko, A. B. & Scully, M. O. Threshold and linewidth of a mirrorless parametric oscillator. *Phys. Rev. Lett.* **84**, 3558–3561 (2000).
21. Lukin, M. D., Matsko, A. B., Fleischhauer, M. & Scully, M. O. Quantum noise and correlations in resonantly enhanced wave mixing based on atomic coherence. *Phys. Rev. Lett.* **82**, 1847–1850 (1999).
22. Artoni, M. & Loudon, R. Quantum theory of optical-pulse propagation through an amplifying slab. *Phys. Rev. A* **57**, 622–628 (1998).
23. Maichen, W., Gaggl, R., Korunsky, E. & Windholz, L. Observation of Phase-Dependent Coherent Population Trapping in Optically Closed Atomic Systems. *Europhys. Lett.* **31**, 189–194 (1995).
24. Lvovsky, A. I., Sanders, B. C. & Tittel, W. Optical quantum memory. *Nat. Photon.* **3**, 706–714 (2009).
25. MacRae, A., Brannan, T., Achal, R. & Lvovsky, A. I. Tomography of a high-purity narrowband photon from a transient atomic collective excitation. *Phys. Rev. Lett.* **109**, 033601 (2012).
26. Zavatta, A., D'Angelo, M., Parigi, V. & Bellini, M. Remote preparation of arbitrary time-encoded single-photon ebits. *Phys. Rev. Lett.* **96**, 020502 (2006).
27. Marcikic, I. *et al*. Time-bin entangled qubits for quantum communication created by femtosecond pulses. *Phys. Rev. A* **66**, 062308 (2002).
28. Simon, C. *et al*. Quantum repeaters with photon pair sources and multimode memories. *Phys. Rev. Lett.* **98**, 190503 (2007).
29. Wu, J.-H., La Rocca, G. C. & Artoni, M. Controlled light-pulse propagation in driven color centers in diamond. *Phys. Rev. B* **77**, 113106 (2008).
30. Wu, J.-H., Artoni, M. & La Rocca, G. C. Decay of stationary light pulses in ultracold atoms. *Phys. Rev. A* **81**, 033822– (2010).

Acknowledgments

The work is supported by the EU through the "Malicia" project (FET - Open grant number: 265522 - 7th Framework Programme), the "Qscale" project (ERA - NET CHIST -ERA) and the ERC Advanced Grant DISQUA, by the Italian-Spanish governments through the MIUR Azione Integrata (grant IT09L244H5), by the Fondo di Ateneo of Brescia University and by the Catalan Government under the contract SGR2009-00347.

Author contributions

A.Z. and M.A. devised the idea of an interface to generate and control frequency bin-entangled states, and wrote the manuscript with input from D.V. and G.L.R. All authors participated in discussions.

Additional information

Competing financial interests: The authors declare no competing financial interests.

How to cite this article: Zavatta, A., Artoni, M., Viscor, D. & La Rocca, G. Manipulating Frequency-Bin Entangled State in Cold Atoms. *Sci. Rep.* **4**, 3941; DOI:10.1038/srep03941 (2014).